ResearchGate

See discussions, stats, and author profiles for this publication at: https://www.researchgate.net/publication/228341460

Synthesis, Characterization, and Application of Novel Polymeric Nanoparticles

ARTICLE *in* MACROMOLECULES · JANUARY 2007

Impact Factor: 5.8 · DOI: 10.1021/ma0613739

CITATIONS
42

READS
71

7 AUTHORS, INCLUDING:

Sandra Warren
UniverCell
4 PUBLICATIONS **65** CITATIONS
SEE PROFILE

Mindaugas Rackaitis
Bridgestone Corporation
36 PUBLICATIONS **699** CITATIONS
SEE PROFILE

Available from: Sandra Warren
Retrieved on: 16 January 2016

Synthesis, Characterization, and Application of Novel Polymeric Nanoparticles

Xiaorong Wang,† James E. Hall, Sandra Warren, James Krom, Jeffery M. Magistrelli, Mindaugas Rackaitis, and Georg G. A. Bohm*

Bridgestone Americas, Center for Research and Technology, 1200 Firestone Parkway, Akron, Ohio 44317

Received June 20, 2006; Revised Manuscript Received October 9, 2006

ABSTRACT: We extended the self-assembly concepts of macromolecules in solutions to create a variety of unique nanosized polymeric core−shell nanoparticles by means which allow scale-up for industrial production. This paper describes the synthesis methods and the mechanisms governing the design of structural features required for a beneficial use as performance-enhancing additives in rubber vulcanizates as well as the performance of such rubber compositions. The nanoparticles were prepared by the polymerization of block copolymers and their self-assembly in solvents into micelles followed by a subsequent stabilization of their structure by core cross-linking. Depending on the type and macrostructure of the block copolymers, the solvent, the concentration, and other process parameters, a variety of core−shell nanoparticles of different shapes (spheres, hollow spheres, ellipsoids, linear and branched strings, etc.) and sizes have been reproducibly synthesized. Most of the nanoparticles were composed of a solid, highly cross-linked core and an elastomeric shell structure. The evolution and structure of the nanoparticles during the different process steps involved were examined and characterized. The unique performance of spherical nanoparticles as performance-enhancing additives and novel reinforcing agents was explored in rubber compounds. It was also shown that the basic spherical or string type nanoparticles can be used as templates for the design of composite structures comprising the basic polymeric nanoparticles and smaller organic, inorganic, or metallic substructures embedded in and attached to the elastomeric shell molecules.

Introduction

Methods that allow the preparation of polymeric nanoparticles with varied and often complex structures and functions have drawn much attention during the past decade. This interest is largely based on the notion that such nanoparticles ranging in size from 10 nm to more than 100 nm may offer enhanced physical, chemical, or biological properties when optimally designed for specific applications. Commercial uses require that they be made reproducibly in relatively high volumes and at a cost commensurate with the value of the benefit they are expected to impart in different applications. However, the development of robust and economically viable processes capable of producing acceptable nanoparticles has been a challenging endeavor.

Polymeric core−shell nanoparticles can be synthesized by at least two different pathways: one involving a sequential synthesis of core and shell structure and the other involving the self-assembly of block copolymers.

The former approach originated from work by a number of researchers[1−13] to produce multiarmed star polymers. One example is the work of Tsitsilianis et al.[7] in which a living polymeric precursor first formed is reacted with a bis-unsaturated monomer such as divinylbenzene (DVB), producing a star-shaped polymer with a small (DVB) core structure. Given the sequence of the synthesis steps this method is often referred to as the "arm first" method. Another approach, called the "core first" method, was first demonstrated by Burchard.[9,10] A bis-unsaturated monomer (DVB) was first polymerized with BuLi in a hydrocarbon solvent at high dilution, producing a stable suspension of small gel particles. The particle surface was then reacted with metal organic functions which served as an initiator for the synthesis of the polystyrene shell structure. Similar techniques were used by Funke[11,12] and more recently by Zheng et al.[13] They too used a multistep process starting with the synthesis of cross-linked nanosize globules by conventional microemulsion copolymerization of polystyrene and divinylbenzene (DVB) and ethylvinylbenzene. In two subsequent steps polybutadiene of up to 17 kg/mol in molecular weight was surface grafted onto the preformed core particle by anionic polymerization after they were washed, dried, and subsequently suspended in hexane. First *n*-BuLi and TMEDA were reacted with the remaining DVB double bonds to generate Li live ends on the surface of the particles, after which butadiene was added to initiate the polymerization of the shell structure.

The second approach involving the self-assembly of block copolymers was used both in the solid state and in polymer solutions.[14−29] Lui et al.,[14,15] for example, reported a process to make polymeric nanoparticles taking advantage of the self-assembly of diblock copolymer in the solid state. Their approach was based on the synthesis of diblock copolymer with a photo-cross-linkable block which allowed them to form an ordered structure of either nanosized spherical or cylindrical domains. After cross-linking the core of these self-assembled structures and dissolving the resultant material in a solvent, they obtained core−shell structured nanospheres[14] and nanofibers.[15] Applying the same concept, Wooley et al.[16−18] used diblock copolymers to form amphiphilic nanoparticles of core−shell structure. In their experiments the micelles were formed in a dilute solution and subsequently stabilized by a cross-linking of the outer shell layer. Similar results were obtained by Akashi et al.[19−22] with comb type polymers prepared by dispersion polymerization of a cross-linkable monomer and a macromonomer. The macromonomer prepared separately and carefully purified[20] prior to its use acted as a steric stabilizer to provide colloidal stability to the micelles formed in a solvent, and eventually it became part of the surface layer of particles. The spherical nanoparticles generated had a core−shell structure with short hydrophilic

* Corresponding author. E-mail: bohmgeorg@bfusa.com.
† E-mail: wangxiaorong@bfusa.com.

10.1021/ma0613739 CCC: $37.00 © 2007 American Chemical Society
Published on Web 01/10/2007

brushes. Many of these approaches may prove difficult to scale up for large volume production because they require fairly complex multistep synthesis, purification, and assembly processes.

Our work focused on means to produce polymeric nanoparticles by commercially viable synthesis processes.[23−29] Given that we were mainly interested in forming core−shell nanoparticles with cores of well-defined size and mechanical as well as thermal stability, we chose to make use of the thermodynamically governed drive of certain heterogeneous molecules such as block copolymers placed in certain solvents to self-assemble into micelles of predetermined size and structure. Living block copolymers can be produced by different synthesis processes such as anionic and living free radical polymerization including reversible addition fragmentation transfer (RAFT) and atom transfer radical polymerization (ATRP) either in a separate process or in conjunction with the micelle-forming step. The thermodynamic properties of such polymer/solvent systems allow the formation of nanoparticles of various shapes such as spheres, strings, etc. Special features such as functional groups, hydrogenation, etc., can also be introduced in the nanoparticle by additional steps undertaken either during the synthesis of the block copolymers or in one or more posttreatment steps performed on the formed nanoparticles.

Experimental Section

Monomers, Solvents, and Synthesis Equipment. Butadiene in hexane (about 22 wt % butadiene), styrene in hexane (about 33 wt % styrene), pure hexane, and *n*-butyllithium in hexane (1.6 M in hexane) were used as supplied under nitrogen from the Firestone Polymer Co. *sec*-Butyllithium (1.4 M in cyclohexane) and triethylamine were obtained from Aldrich. A dilithium initiator was prepared in situ according to the following procedure. Equal molar amounts of triethylamine and *sec*-butyllithium were first charged to a clean, dry, nitrogen-purged closed bottle. Then 1,3-diisopropenylbenzene was added at a 1:2 molar ratio to the *sec*-butyllithium. The bottle was heated with agitation for 1.5 h at 50 °C. The resultant product was used as the dilithium initiator. Technical grade divinylbenzene (Aldrich) containing mixture of isomers (80%) as well as isomers of ethylvinylbenzene was passed through a column comprising a proprietary activated alumina based inhibitor remover (Aldrich) and calcium hydride under nitrogen before use. Monomer *tert*-butylstyrene was also obtained from Aldrich and reacted with activated alumina and calcium hydride under nitrogen. Neat oligomeric oxalanylpropanes obtained from the Firestone Polymer Co. were similarly treated and used as a 1.6 M solution in hexane and stored over calcium hydride. Other solvents such as 2-propanol, acetone, toluene, and the antioxidant butylated hydroxytoluene (BHT) were used as received. A 7.6 L reactor (Chemineer Inc.) equipped with a pitch blade impeller was used for most of the synthesis work. The nanoparticles of this study were all made by anionic polymerization in this high-pressure closed reactor.

Synthesis of Spherical Nanoparticles. Option A. The reactor was first charged with 0.508 kg of hexane and then 1.043 kg of the butadiene/hexane blend (22 wt % of butadiene). The batch was then heated to 57 °C. After the temperature stabilized, polymerization was initiated by adding 5.0 mL of 1.6 M *n*-butyllithium in hexane. After 2 h, the reactor was charged with 0.66 kg of a styrene/hexane blend that contained 33 wt % styrene. After an additional 2 h reaction, the reactor was charged with 1.81 kg of hexane and then 50 mL of divinylbenzene. A batch temperature of 57 °C was maintained duration the entire polymerization process. The product was then dropped into a solution of 2-propanol and BHT and subsequently dried in vacuum. The GPC analysis of the product showed two distinct peaks. One was from the micelle nanoparticles (∼95%), and the other was from some unreacted diblock copolymer (∼5%). The molecular weight of the diblock was about 49.4 kg/mol. The polydispersity of the nanoparticles was 1.15.

Synthesis of Spherical Nanoparticles. Option B. The reactor was first charged with 0.508 kg of hexane and then 1.043 kg of the butadiene/hexane blend (22 wt % of butadiene). The batch was then heated to 57 °C. After the temperature stabilized, polymerization was initiated by adding 5.0 mL of 1.6 M *n*-butyllithium in hexane. After 2 h, the reactor was cooled to 20 °C and then charged with 1.7 mL of the 1.6 M *n*-butyllithium solution and following that with a blend of 0.66 kg of styrene/hexane (33 wt % of styrene) and 50 mL of divinylbenzene. The reactor was maintained at 57 °C for another 2 h period. After that, the living polymer was terminated by dropping it into a solution of 2-propanol and BHT at a ratio of 99/1 and then dried in vacuum.

Synthesis of Flower Type Nanoparticles. The polymerization reactor equipped with external jacket heating and internal agitation was used for the preparation. The reactor was first charged with 0.52 kg of hexane and 1 kg of a butadiene/hexane blend (22 wt % butadiene). The batch was then heated to 57 °C. After the temperature stabilized, polymerization was initiated by adding 16 mL of a 0.5 M solution of the dilithium initiator in hexane. The dilithium solution was made according to the procedure described earlier. The batch temperature was maintained at 57 °C for the duration of the polymerization. After 2 h, the reactor was charged with 0.7 kg of a styrene/hexane blend (33 wt % of styrene). After an additional 2 h reaction, the reactor was charged with 2.8 kg of hexane and then 50 mL of divinylbenzene (DVB). The temperature was maintained at 57 °C for another 2 h period. The reactor was then discharged, and the product was dropped into a 95/5/1 blend of acetone/2-propanol/BHT and subsequently dried in vacuum.

Synthesis of Hollow Nanoparticles. The reactor was first charged with 1.134 kg of hexane and then 0.68 kg of the styrene/hexane blend (33 wt % styrene) and the batch heated to 85 °C. After the temperature stabilized, polymerization was initiated by adding 1.6 mL of 1.6 M oligomeric oxalanylpropane in hexane and 8 mL of 1.6 M *n*-butyllithium in hexane. The batch temperature was maintained at 85 °C for 20 min. Then 1.0 mL of 2-propanol was added to terminate the polymerization. This procedure was used to prepare the PS for first forming the globules later used as templates for generating the hollow particles. After 17 min the reactor was charged with 0.635 kg of a butadiene/hexane blend (22 wt % of butadiene) and then 8 mL of 1.6 M *n*-butyllithium to reinitiate the polymerization. 25 min later the reactor was charged with 0.09 kg of a styrene/hexane blend of (33 wt % styrene). This procedure formed BD/S block copolymers having a short PS block to prevent the formation of separate micelles but causing the block copolymer molecules to decorate themselves around the PS globules. The reactor was then cooled to 40 °C, and 20 min later 100 mL of divinylbenzene was added to the reactor. The reactor temperature was then maintained at 40 °C for another 1.5 h, after which the reaction was terminated by dropping the batch into a 95/4/ 1 blend of toluene, 2-propanol, and BHT. The solution was then precipitated by adding extra hexane. Since PS is insoluble in hexane at 23 °C it precipitated, while the hollow particles comprising the polybutadiene brushes remained soluble. The soluble nanoparticles particles were then collected and dried in vacuum.

Synthesis of Linear Nanostrings. The reactor was charged with 1.19 kg of a butadiene/hexane blend (22 wt % butadiene) and heated to 57 °C. After the temperature had stabilized, polymerization was initiated with 10.2 mL of a 1.5 M butyllithium/hexane solution. The batch temperature was maintained at 57 °C for the duration of the polymerization. After 2 h, the reactor was charged with 1.81 kg of a styrene/hexane blend of (33 wt % styrene). After an additional 2 h reaction time, the reactor was charged with 55 mL of divinylbenzene. 10 min later the agitation was stopped, and the temperature was maintained at 57 °C for an additional 2 h. The batch was then discharged into a 95/4/1 blend of acetone, 2-propanol, and BHT and subsequently dried in vacuum.

Synthesis of Branched Nanostrings. The reactor was first charged with 1.814 kg hexane and 0.522 kg of a butadiene/hexane solution (22 wt % butadiene) and the reactor heated to 57 °C. When the batch reached 57 °C, 10 mL of 0.5 M dilithium solution and 1 mL of 1.6 M *n*-butyllithium were added. After 2 h, 0.68 kg of a styrene/hexane blend (33 wt % styrene) was added to the reactor. A temperature peak of about 70 °C was observed after 20 min due

Table 1. Characterization of Polymeric Nanoparticles

sample	PBD shell M_n (kg/mol)	shell M_w/M_n	PBD/PS ratio in particle	DVB content in particle (%)	particle purity (%)	particle diameter (nm)	particle length (nm)	particle poly-dispersity
spherical nanoparticles								
by option A	24.7	1.05	50/50	8	95.0	20	n/a	1.15
by option B	24.9	1.03	50/50	8	99.0	20	n/a	1.12
flower-type nanoparticles	56.7	1.04	50/50	8	82.0	25	n/a	1.10
hollow nanoparticles	26.8	1.05	42/58	46	90.0	30	n/a	1.16
nanostrings								
linear structure	14.2	1.03	30/70	6	>95	20	1000−10000	n/a
branched structure	n/a	n/a	34/66	8	>95	20	1000−10000	n/a
nanocomposite particle	24.9	1.05	50/50	8	90.0	20	n/a	1.15

to the exothermic reaction. After another 1.5 h, 50 mL of divinylbenzene (DVB) was added, and the solution was allowed to react for an additional 1.5 h The batch was then dropped into a 95/4/1 blend of acetone, 2-propanol, and BHT. The polymeric product was then filtered through a cheese cloth and dried in vacuum.

Synthesis of Nanocomposites. A 2000 mL three-neck round-bottom flask was used for the synthesis. The middle neck was used for mechanical stirring. The left neck was used for charging the various materials and the right neck for nitrogen purging and temperature measurements. 70 g of diisopropyl azocarboxylate (from Aldrich) and 1200 g of a toluene/nanoparticle solution containing 8 wt % spherical nanoparticles prepared by option B described earlier were all added into the flask. The flask was then placed into a silicon oil bath, heated to 110 °C, and held at that temperature for 7 h. When the reaction product was dropped into hexane, a light-yellow product precipitated from the solution. After redissolving it in toluene and reprecipitating the solution in hexane five consecutive times, the product was dried in vacuum. ^{13}C NMR comparison of the carbonyl and aromatic groups showed that the product contained about 85 parts of chemical bonded diisopropyl azodicarboxylate based on 100 parts (by weight) of the original polymer. The product was soluble in methanol, ethanol, 2-propanol, THF, chloroform, and toluene but not soluble in hexane and cyclohexane. The azo-dicarboxylated nanoparticles were then redissolved in toluene and further diluted to about a 3% concentration. Then 10 parts of a $Cd(Ac)_2$/MeOH solution (3 wt % $Cd(Ac)_2$) were charged to 100 parts of the solution. The solution was transparent and colorless. H_2S gas was then bubbled through the solution to fully convert the Cd ions to CdS. The solution was then purged with nitrogen to remove excess H_2S. The resulting solution was yellow, but no macroscopic precipitation of CdS occurred from the solution. The product was then placed in a vacuum oven at 50 °C, yielding a film of polymeric nanocomposite particles. The film was yellow and transparent to light.

Characterization of Nanoparticles. Molecular weights were determined by gel permeation chromatography (GPC) using Waters HSGPC equipment and tetrahydrofuran (THF) as solvent. Solid samples were weighed, dissolved in THF, and filtered before injection into the GPC column. The column was calibrated using polystyrene standards, and the averaged molecular weight of the sample was estimated on the basis of these standards and a universal calibration curve.

The polymer microstructure such as vinyl and styrene content was determined by ^1H NMR measurement. A Varian Gemini 300 NMR spectrometer was used. The polymers were dissolved in a deuterated solvent ($CDCl_3$) and filtered before being transferred them into a NMR tube for measurement.

A DSC 2910 differential scanning calorimeter was used to determine the T_g of the polymer. The temperature at which the inflection point of heat capacity ($C_p = f(T)$) occurs was used as a measure of T_g. The temperature and the heat flow signals were calibrated with indium. The temperature scan rate was 10 °C/min.

Electron microscopic observations were carried out with a Phillips CM-12 transmission electron microscope (TEM) and a Hitachi S-4800 scanning electron microscope in STEM mode. About 10 mL of the polymer solution was taken from a final polymerization batch and further diluted with hexane solvent to about 10^{-4} wt % of the polymer solid. A drop of the diluted solution was then deposited on a carbon-coated microgrid. After the solvent was evaporated, the grid was stained with OsO_4 and examined by electron microscopy.

Atomic force microscopic (AFM) observation was carried out with a Dimension 3000 microscope made by Digital Instruments. The AFM was used in tapping mode with an etched silicon tips. A small drop of the diluted solution ($\sim 10^{-4}$ wt %) was placed on a newly cleaved graphite surface of about 10 × 10 mm size. The examination commenced when the solvent had completely evaporated.

Preparation of Rubber Compounds. Rubber compositions were prepared using commonly accepted procedures. A master batch was formulated with 100 phr polymer, varied amounts (0−70 phr) of N343 carbon black, varied amounts (0−75 phr) of polymeric nanoparticles, and different processing aids including 3 phr zinc oxide, 2 phr hydrocarbon resin tackifier, 0.95 phr antioxidant (Santo flex 13), 2 phr stearic acid, and 1 phr wax. The unit "phr" refers to "parts per hundred rubber". Mixing was performed in a 300 g Brabender mixer using a mixing speed of 60 rpm. At time zero, the polymer was charged to the mixer, preheated to an initial temperature of 110 °C. The remaining ingredients were added at $t = 0.5$ min. The batch was removed at $t = 5$ min when the temperature of the stock approached 150 °C. The master batch was later mixed with curatives in the Brabender mixer at 60 rpm to form a final stock. The curatives used were 2.1 phr sulfur, 1.4 phr cyclohexylbenzothiazole sulfenamide (accelerator), and 0.2 phr diphenylguanidine (accelerator). The master batch was added to the mixer held at 75 °C at time zero, the curatives were then charged at $t = 0.5$ min, and the final batch was removed from the mixer at $t = 1.3$ min when the temperature of the stock reached ~90 °C. The final stock was sheeted on a two-roll mill at 60 °C and cured in molds at 165 °C for 15 min.

Measurement of Physical and Rheological Properties. Measurement of dynamic moduli (G' and G'') of rubber compounds reinforced with nanoparticles were carried out at different strain amplitudes using a Rheometrics ARES strain-controlled rheometer equipped with dual 200 and 2000 g cm force rebalance transducers and controlled using RSI Orchestrator V6.56 software. Strain sweeps were done at 5 Hz and 30 °C. The test specimen was a cylinder 9.5 mm in diameter and 15 mm in length. It was glued to a pair of parallel plates using superglue and then mounted in the instrument. For temperature sweeps the test specimen was a strip 30 mm in length and 15 mm wide mounted between a pair of strip fixtures. The testing conditions were 5 Hz at 2% strain amplitude. Tensile strength measurements were carried under conditions described in ASTM-D 412 at 22 °C using a ring, 25.4 mm in diameter and having a thickness and width of 1.9 and 1.27 mm, respectively.

Results and Discussion

Synthesis and Structure of Nanoparticles. In the following we will describe the detailed process steps involved in the synthesis of some of these above referred to polymeric nanoparticle based on the use of styrene/butadiene block copolymers,

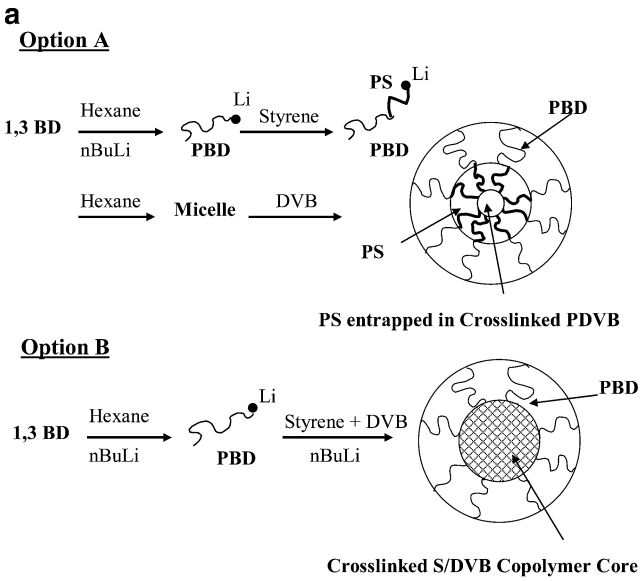

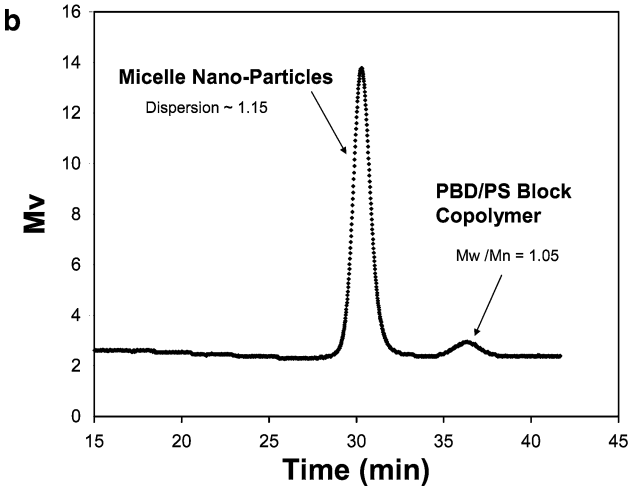

Figure 1. (a) Synthesis of spherical nanoparticles. Option A: core cross-linking by addition of divinylbenzene to living PBD/PS diblock aggregates. Option B: core cross-linking by copolymerization of styrene and divinylbenzene. (b) GPC spectrum of the final product according to the process shown in option A.

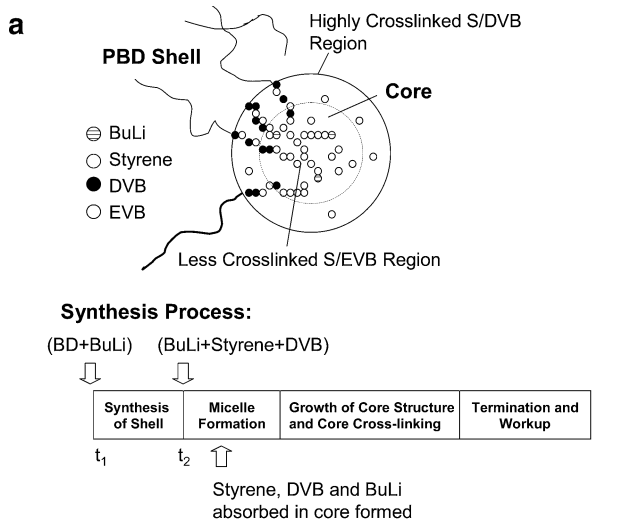

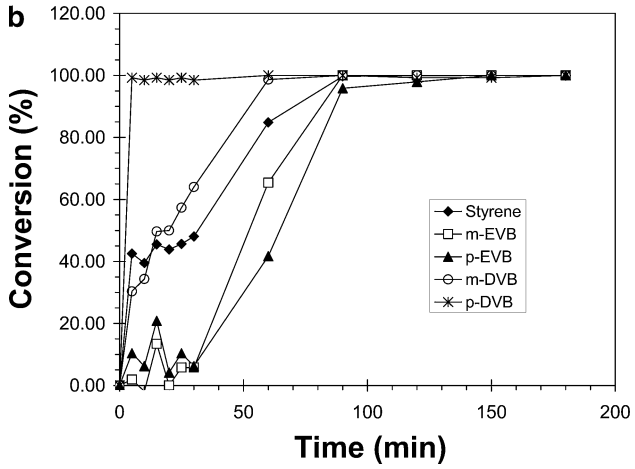

Figure 2. Dynamics of core formation: (a) sequence of events taking place during the core formation, which result in the formation of the core of a less cross-linked region and a highly cross-linked region; (b) monomer conversions during the core formation.

since the extension to other systems is then straightforward. The composition and structure information on the nanoparticles produced are summarized in Table 1.

a. Spherical Nanoparticle. A diblock copolymer with a molecular weight of 50 kg/mol and a 50/50 BD/styrene weight ratio was synthesized using lithium-initiated living anionic polymerization by a sequential addition of first butadiene and then styrene after all the butadiene has been polymerized, as shown in Figure 1, option A. In a hexane solution of about 12% solid, this living diblock aggregate forms spherical micelles, with the styrene block directed toward the center of the micelle and the butadiene block as tail extending therefrom. This occurs because the polystyrene blocks of the copolymer are largely insoluble in hexane whereas the polybutadiene blocks are very soluble in this solvent.

After forming the micelles, 8 wt % (of the diblock polymer) divinylbenzene (DVB) was added. The divinylbenzene, having a strong affinity for styrene, is diffusing to the center of the micelles where it reacts with the living anions on the polystyrene chain ends to polymerize a poly(divinybenzene) adduct which subsequently undergoes inter- and intramolecular cross-linking via the slower reacting second double bonds, thus forming a highly cross-linked region in the polystyrene core of the nanoparticle. Rheological measurements performed on the nanoparticles showed the existence of a hysteresis peak at about 80 °C, which indicates that the cross-linked, DVB-rich core region did not intermix completely with the styrene-rich part of the core. Nevertheless, the cross-linking of the nanoparticle core permanently stabilizes the shape of the self-assembled micelle structure.

The synthesis process involving these steps produces nanoparticles of a narrow size distribution with the data listed in Table 1. The GPC spectrum of the final product shows two distinct peaks (see Figure 2b). The larger one is from the micelle nanoparticles (~95%) and the other from unreacted diblock copolymer (~5%) which did not get incorporated in the micelle structures due to impurities introduced by the sequential charging of solvent and monomers during anionic polymerization. The polydispersity of the micelle nanoparticles is about 1.15, and the molecular weight distribution M_w/M_n of the original diblock copolymer is 1.05.

Alternatively, the cross-linking of the core can also be accomplished by copolymerizing styrene and divinylbenzene instead of just styrene during the formation of the block copolymer as shown in Figure 1, option B. This option provides an opportunity to achieve a more uniform cross-link distribution in the core region and to meet specific application needs by the

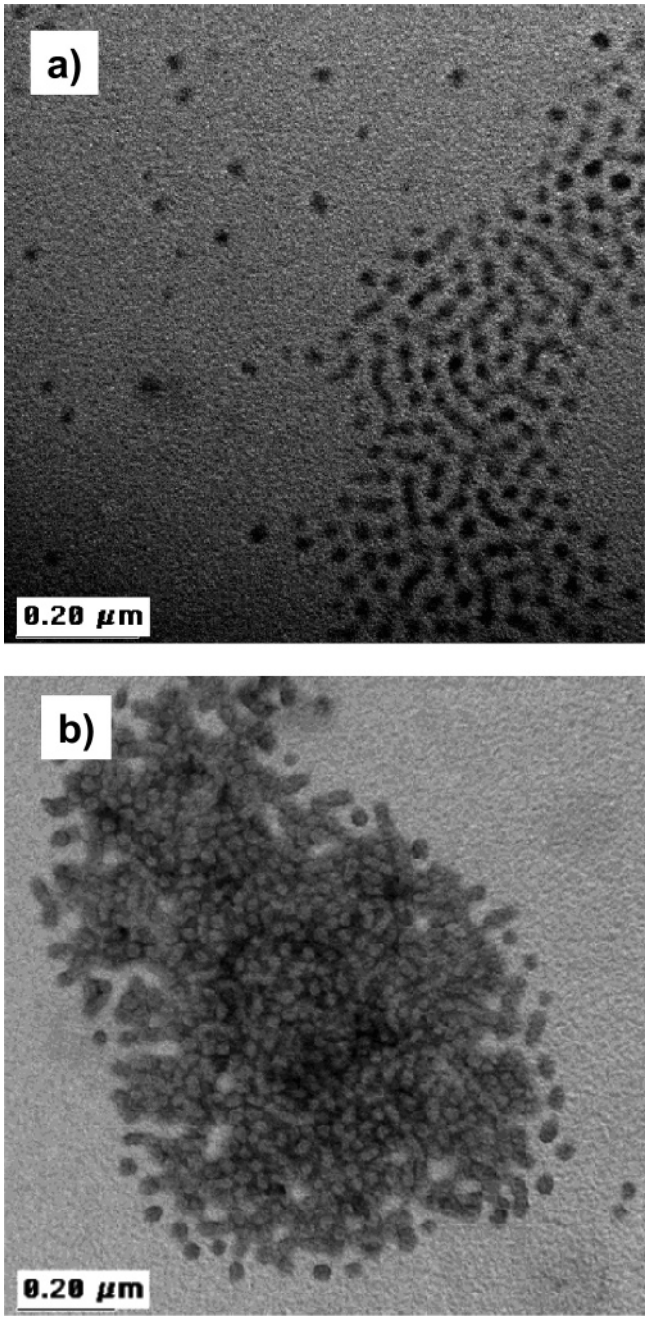

Figure 3. TEM photographs of polymeric spherical nanoparticles: (a) PS/PBD core−shell nanoparticles; (b) hydrogenated PS/PBD nanoparticles.

appropriate selection of the monomers, their addition sequence, the presence or absence of additional BuLi, and certain process parameters. In the case of the BD/S/DVB-based nanoparticles we were able to vary the core T_g from about from 100 to above 280 °C. As stated, the dynamics of core formation has significant bearing on the structure, thermal stability, and ultimately the performance of the nanoparticles, and we thus investigated the consumption of styrene and DVB including its isomers and impurities contained in technical grade DVB during the core formation phase.

Figure 2 shows the results obtained and the proposed sequence of events taking place. The BD shell molecules polymerized during t_1 are fully soluble in hexane, but shortly after S/DVB segments of a certain length have grown onto the shell molecules starting at $t_2 = 0$ the concentration of block copolymer formed exceeds the critical micelle concentration at

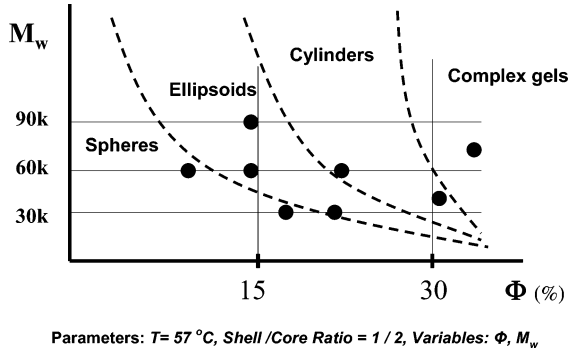

Figure 4. Phase diagram of PS/PBD diblock copolymers in hexane.

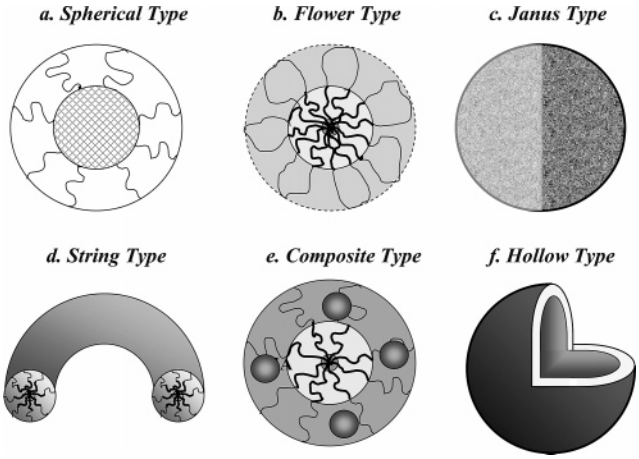

Figure 5. Nanoparticles of different shape and structure produced in a batch process using our technology.

the temperature of the experiment and micelles will begin to form. Our studies show that micelles form relatively quickly perhaps aided by clusters of living BD shell molecules held together in the solvent by ionic attraction between the anions located at the chain ends. These clusters are likely preserved during the early growth of the S/DVB adducts and strengthened by the additional BuLi we added at $t_2 = 0$. However, given the small diffusion coefficient of high molecular weight copolymers, we anticipated that the time required to reach equilibrium in micelle formation would take a longer time. The concentrations of styrene, DVB, and BuLi in the micelle core region will tend to be higher than in the solvent and be governed by μ_i(core) = μ_i(solvent), the thermodynamic equilibrium.

The DVB we use is technical grade from Aldrich (product no. 414565) and contains four components: *m*-EVB (∼10%), *p*-EVB (∼9%), *m*-DVB (∼57%), and *p*-DVB (∼24%). As the lengths of the S/DVB adducts continue to grow, the micelles will grow in size and perfection. As shown in the monomer conversion graph of Figure 2b, *p*-DVB copolymerizes more quickly owing to its larger reaction constant,[6] and hence the polymer segments starting to form at $t_2 = 0$ are very rich in DVB. As *p*-DVB is being consumed, *m*-DVB and the ethylvinylbenzene isomers are being copolymerized as well. Inter- and intramolecular cross-linking of the core structure through the second double bonds of the copolymerized DVB will also take place, albeit at a slower rate. The size and distribution of the core segments relative to each other change during t_2 based on the thermodynamics of the changing system and the process kinetics taking into account the growing chains, the monomers and BuLi concentration in the core phase, and the cross-linking of the chain segments.

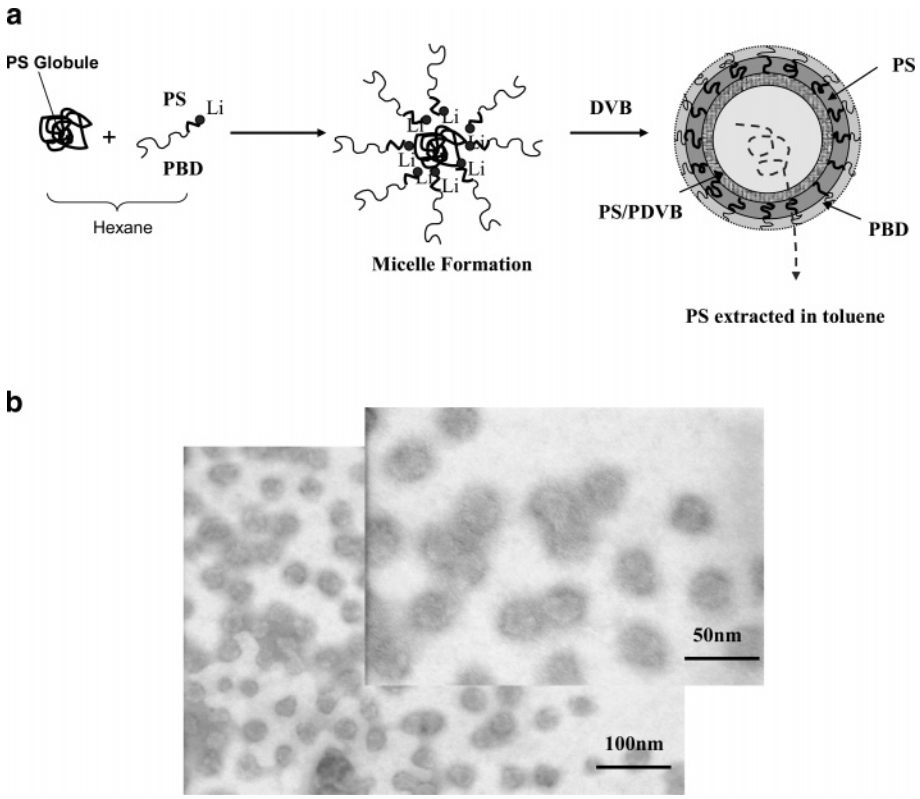

Figure 6. (a) Synthesis of hollow nanoparticles showing process steps. (b) TEM images of hollow particles produced.

Given this process sequence, we have to assume that the outer core region of the polymer produced in this experiment is more densely cross-linked than the core center due to the DVB concentration gradient. We also have to conclude that at some time in the process when significant cross-linking has occurred in the outer core region the polymerization of nanoparticles slows down and eventually stops as core cross-linking restricts core growth even if unreacted monomer (S, DVB, etc.) is present in the solvent.

The shape and size of the nanoparticles can be seen in the TEM micrograph of Figure 3. This analysis involved a hexane solution of the final product at about a 10^{-5} wt % concentration. A drop of the diluted hexane solution was coated onto a carbon-coated copper microgrid. After the solvent was vaporized, the sample was stained with RuO_4 and examined by TEM. As can be seen, the nanoparticles are spherical and about 20 nm in diameter (Figure 3a). If the product is hydrogenated, an even sharper image is obtained (Figure 3b).

The micellization of diblock copolymers is an enthalpically driven process with the negative Gibbs free energy of eq 1

$$\Delta G^{o} = \Delta H^{o} - T\Delta S^{o} \qquad (1)$$

dominated by the negative ΔH^{o}, which is the result of a stronger polymer/polymer interaction in the micelle cores as compared to polymer/solvent and solvent/solvent interaction in the absence of micelles. The change in entropy is also negative and thus unfavorable to the formation of micelles, but $T\Delta S^{o}$ is much smaller than ΔH^{o}. By changing the thermodynamic conditions governing the self-assembly of BD/S block copolymers, one would thus expect that micelles of different structures be generated. The results of theoretical efforts to predict micelle structure from the characteristics of the block copolymers have been reviewed by several authors.[30,31]

The formation of various micelle shapes which can be produced from BD/S block copolymers in a given solvent depends on the volume fractions of the components (ϕ_j, $i = 1$, 2), the miscibility of the components as expressed by the $\chi_{ij}N_j$ parameters, where χ is the interaction parameter and N is the degree of polymerization, and on the shell to core volume fraction. To explore this, we carried out experiments in which the molecular weight of the block copolymers was varied as well as the block copolymer concentration in hexane while keeping the polymerization temperature and the core-to-shell weight ratio of the block copolymers constant with the results shown in Figure 4. As one can see, for a block copolymer with a molecular weight of about 60 kg/mol and a BD/S ratio of 1/2, spherical nanoparticles are formed at relatively low polymer concentrations, e.g., at $\phi < 12$ vol %. As the concentration ϕ increased to about 12 but still below 20 vol %, the preferred morphology was found to be ellipsoids. At still higher concentration of about 22 vol %, the morphology changed to cylinders. Above 30 vol % only complex gels were observed. Molecular weight also affected particle characteristics but to a lesser degree than ϕ. At block copolymer concentration of about 15 vol %, spherical nanoparticles are mostly formed if the molecular weight of the diblock copolymer is smaller than 40 kg/mol. As the molecular weight increases to above 60 kg/mol but still below 120 kg/mol, the system changes its morphology to ellipsoids and short cylinders. Above 120 kg/mol, the system forms cylinders. In general, increasing the temperature or increasing the shell block length favors the formation of spheres. Increasing the core block length or the concentration favors the formation of cylinders. On the basis of this information as well as process changes, we prepared a variety of spherical as well as nonspherical nanoparticles shown schematically in Figure 5 and discussed in the following.

b. Flower Type Nanoparticle. In order to avoid the presence of end groups in the brush structure of spherical particles, a micelle can also be formed from a living S/BD/S triblock polymer which will form a flower-like nanoparticle with looped

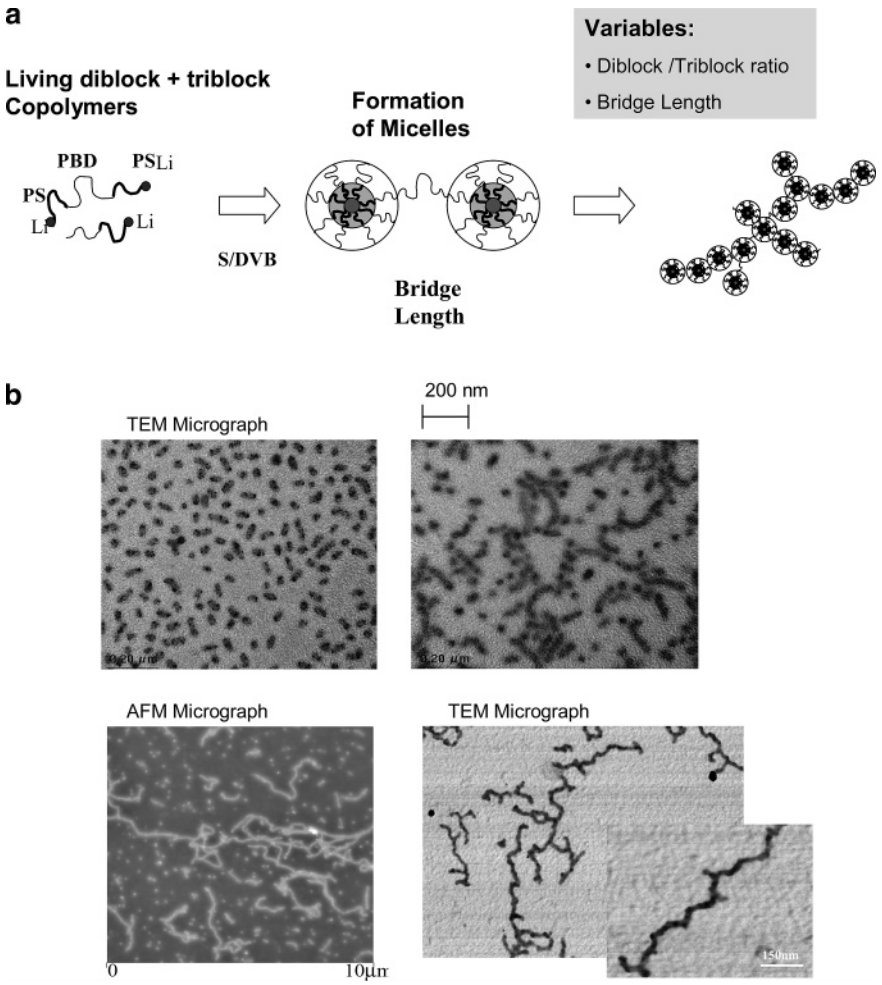

Figure 7. (a) Synthesis of linear and branched string type nanoparticles. (b) Microscopic images of ellipsoids, cylinders, and linear and branched nanostrings.

polybutadiene chains such as shown schematically in picture b of Figure 5. The triblock copolymer is formed by living anionic polymerization initiated by a dilithium catalyst, in which styrene monomer is added to a completely polymerized polybutadiene section, positioning the live ends on both styrene blocks. Because the middle block is soluble in hexane and the two living end blocks are less soluble in hexane, the polymer chains aggregate in hexane solution to form micelles of flower-like structures. The micelle core of this polymeric nanoparticle can also be cross-linked by the means described earlier involving either a copolymerization of styrene and divinylbenzene during the micelle formation step or an addition of divinylbenzene after the micelles have formed.

c. Janus Type Nanoparticles. The shell structure of spherical nanoparticles can also be designed to have two different brushes. For example, one may be polybutadiene and the other poly(*tert*-butylstyrene). The process then involves separately polymerizing alkylbenzene monomers (such as styrene and *tert*-butylstyrene) and conjugated diene monomers (such as butadiene) in hexane solvent to form two types of block copolymers, such as the polystyrene-*b*-polybutadiene and polystyrene-*b*-poly(*tert*-butylstyrene). In both cases the living species are located at the end of the PS block. Combining the two block copolymers in hexane causes micelle-like structures to form with the PS block directed toward the center of the micelles and the hexane-soluble blocks as tails extending therefrom. After forming the micelles, a cross-linking agent (such as divinylbenzene) is added to the system to stabilize the nanoparticles by a link up and subsequent cross-linking of the core segments.

Upon phase separation of the outer blocks induced by an appropriate selection of a solvent system and assuming that the core diameter is much smaller than the shell length, two situations can be anticipated. The first can be expected when the phase separation is incomplete, in which case a spinodel type phase separation may occur at the particle surface. The second one is more interesting and should occur when the phase separation is complete. Then a Janus-like surface morphology should form with two surface regions having different properties, as schematically shown in picture c of Figure 5. Complete phase separation can be achieved by converting the polybutadiene block into more polar structures by steps undertaken either during the synthesis of the block copolymers or in one or more posttreatment steps performed on the formed nanoparticles (e.g., by the posttreatment described in section f). We are carrying out additional measurements on these Janus type particles and expect to publish the results when completed.

d. Hollow Type Nanoparticle. The synthesis of a hollow nanoparticle was achieved by a modified procedure that comprises forming nanosized polystyrene globules in hexane in which the globules are essentially insoluble. Then styrene−butadiene diblock copolymers with an anionic living end on the styrene block are added where they assemble as micelles surrounding the preformed polystyrene globules, as shown in Figure 6a. The enlarged micelle is then comprised of an outer shell made of polybutadiene brush, an inner polystyrene shell containing the Li, and the globular core made of polystyrene. The anionic live ends in the inner shell may then be cross-linked by divinylbenzene as described earlier. In the final step

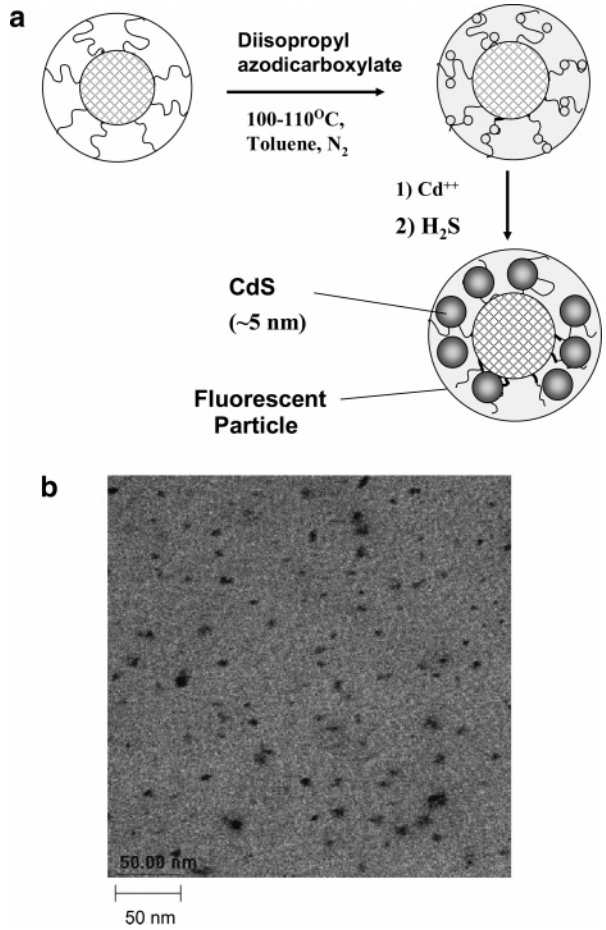

Figure 8. (a) Formation of nanoparticle composites using polymeric nanoparticles as templates in initial process step. (b) TEM image of composite nanoparticles. In the image, only CdS crystals are observable as small dark spots since the polymer part of the particles was not stained and is therefore not visible.

the polystyrene core molecules are extracted in a suitable hydrocarbon solvent such as toluene with the result that a hollow nanoparticle such as shown schematically in picture f of Figure 5 is formed. The overall size and the void space in the particle can be tailored by the solvent, the molecular weight of the polystyrene used for the formation of the original globules, the macrostructure of the diblock copolymers, and a number of other process parameters.

The particles formed are uniform in shape, have a narrow size distribution, and cover a wide size range. The process permits additional particle design features such as a modification of the outer or inner surfaces by functional groups, the use of monomers other than butadiene and styrene, etc. A TEM picture of a hollow nanoparticle prepared by this method is also shown in Figure 6b. It involved applying a drop of a dilute hexane suspension of the nanoparticles on a carbon-coated copper microgrid and the subsequent staining of the particles. The donut-like appearance, similar to those seen with red blood cells, is consistent with the image of a collapsed hollow sphere on a flat surface. The size of the particles in the image is 30−40 nm.

e. Nanostrings. The forming of nanostrings has been of great interest to us as one can anticipate many useful applications of such structures as reinforcing particles for rubber compounds, etc. They can be synthesized by two different routes. The first involves the use of relatively high molecular weight diblock copolymers of high S/BD ratio at relatively high solute concentration, as suggested by the phase diagram of Figure 4. Another potentially more promising and technically more useful approach is to use a mixture of di- and triblock copolymers in the micelle formation process. We found that by varying the ratio of triblock to diblock copolymers as well as the molecular weight of the BD center block in the triblock copolymer, we could form nonspherical particles varying in shape from ellipsoids to long linear or branched strings and to larger dendritic structures, as shown in Figure 7. Linear as well as branched strings having a diameter of about 30 nm and a length of up to 10 μm can be produced. We believe that the shape changes are induced by a bridging between micelles by triblock copolymers. The polystyrene cores of the nanostrings formed are directed toward the center of the micelles with the butadiene brush structure extending therefrom, as shown schematically in picture d of Figure 5. These particles too can be stabilized by core cross-linking involving divinylbenzene and the Li anions located on the ends of the polystyrene blocks as has been discussed earlier. The AFM micrographs were prepared by first redispersing the nanostrings in a very dilute toluene solution and then spin-casting a drop on a newly cleaved graphite surface.

f. Nanocomposites: Nanoparticles as Templates for Organic, Inorganic, or Metallic Substructures. For the design of nanoscale composite particles, we chose spherical nanoparticles of the type described earlier as a primary building blocks or templates and then introducing appropriate functional groups in the shell structure to initiate reactions which permit inorganic or metallic structures to be added. Depending on the functional group and whether it is desired to have it at chain ends or randomly located on the elastomeric shell structure, this can be done either during the synthesis of the diblock copolymers or as part of a posttreatment following the making of the nanoparticles. To illustrate this method, we reacted shape-stabilized spherical nanoparticles of Figure 1 with diisopropylazo dicarboxylate (DIAD) while the particles were suspended in toluene. As shown schematically in Figure 8, the azo groups of DIAD will react at random with the unsaturations of the PBD brush. The pending carboxyl and amine functionalities can then be used in subsequent reactions to form organic, inorganic, or metallic inclusions located within the preformed nanoparticle. In the case displayed in Figure 8 the carboxyl and amine groups are further reacted with Cd^{2+} and then H_2S to form CdS crystals ~5−10 nm in diameter within the outer layer of the nanoparticle. Since CdS can be readily excited giving off fluorescent light, we created a composite nanoparticle which could be used as a tracer in the biomedical field to name one possible application. A TEM micrograph of a relatively thin layer made up of these composite nanoparticles can be seen in Figure 8b where only the CdS crystals are observable as small dark spots. The polymer part of the particle was not stained and is therefore not visible.

Reinforcement and Performance Tuning of Rubber Compounds by Core−Shell Nanoparticles. Rubber compounds are traditionally reinforced with carbon black or silica. As the hard cores of the earlier described spherical nanoparticles are about the same size or smaller than the primary carbon black particles, we were keenly interested in exploring the reinforcing capability of these new materials. This was done by comparing the stress−strain properties of two sulfur vulcanized rubber compounds: one reinforced with carbon black (N343) (compound A) and the other with spherical polymeric nanoparticles (compound B). Polybutadiene (PBD) with a molecular weight of M_w = 150 kg/mol (M_w/M_n = 1.1) identical in microstructure (cis/trans/vinyl = 33/56/11%) to the PBD brush segments of the nanoparticles was used as the host polymer, and the composition of the two rubber compounds is shown in the table inserted in

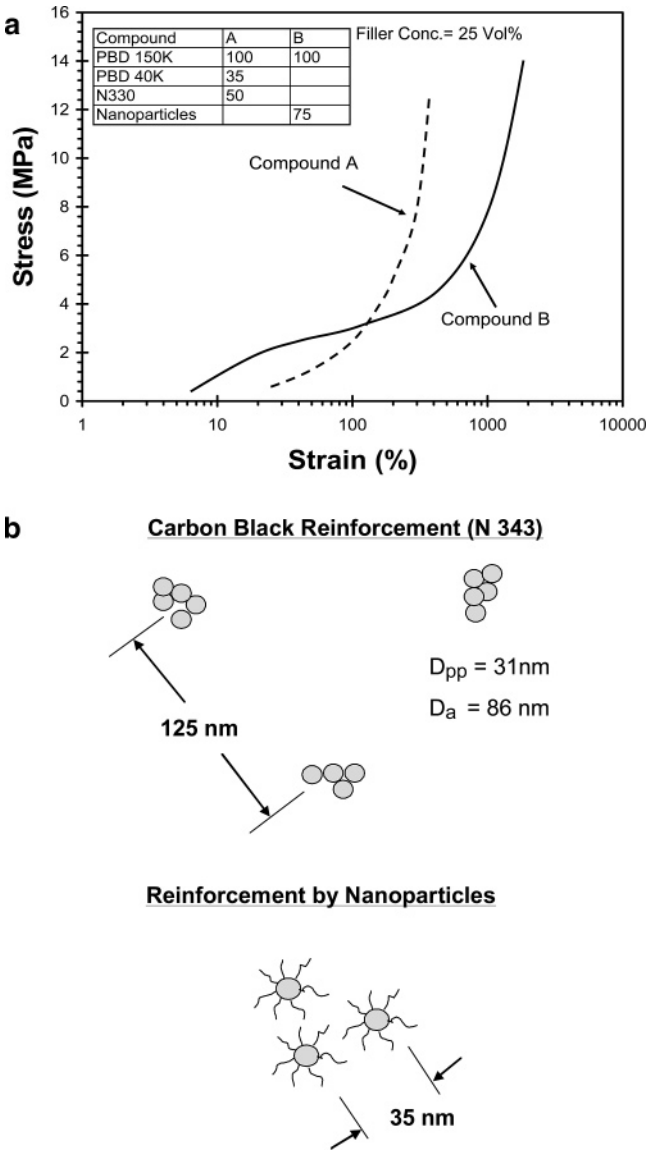

Figure 9. (a) Stress−strain performance comparison of two sulfur vulcanized polybutadiene rubber compounds: one reinforced with carbon black (N343) and the other with spherical PBD/PS nanoparticles, both comprising an identical volume fraction of reinforcing filler. (b) An interpretation regarding the reinforcement mechanism.

Figure 9a. 35 phr of PBD (M_w = 40 kg/mol) was added to compound A to match the PBD brush molecules of the polymeric nanoparticles in compound B. The nanoparticles used in this experiment had a polystyrene/DVB core diameter of 35 nm, an overall diameter of 50 nm, and an equal molar concentration of PBD and polystyrene. As a result, the volume fraction of carbon black in compound A (16 vol %) was nearly equal to that of the reinforcing core portion of the nanoparticles in compound B.

As shown in Figure 9, the compound reinforced with polymeric nanoparticles has a significantly higher modulus at low strains and superior failure properties such as equal tensile strength, higher elongation at break, and higher tensile break energy (tensile strength multiplied by the elongation to break) compared to those of the carbon-filled compound.

An interpretation of this result requires recognition of the differences between the two reinforcing fillers used in compounds A and B, particularly as related to their structure, dispersion, and linkage to the rubber network they are embedded in. With regard to structure and dispersion N343 carbon black

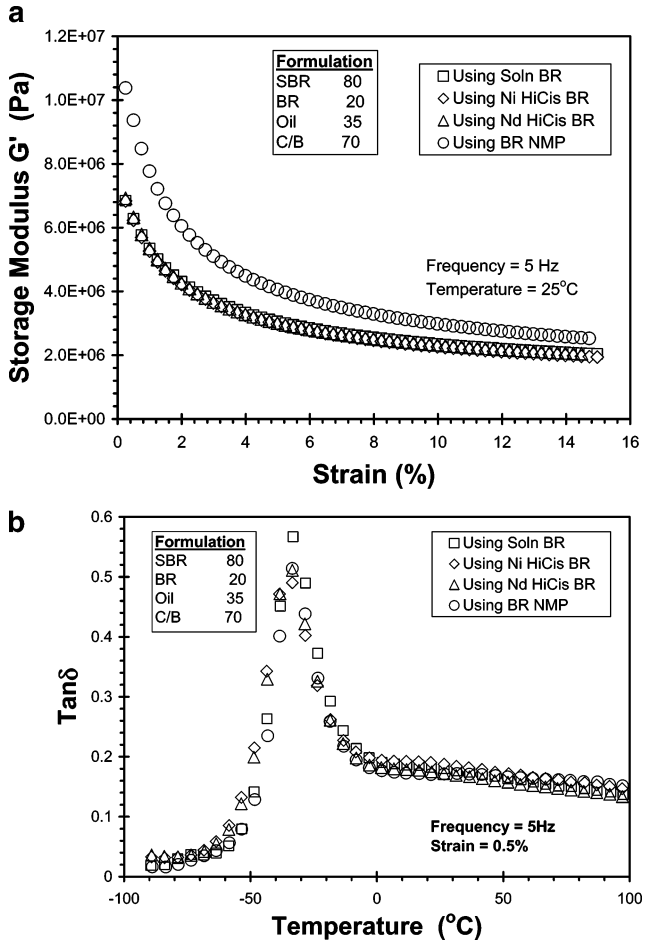

Figure 10. Application of polymeric nanoparticles as additive to sulfur-cured rubber compounds for the tuning of dynamic physical properties: (a) strain sweep plot and (b) temperature sweep plot.

aggregates ~180 nm in size are made up of several 25 nm sized primary particles permanently fused together during the manufacturing process. Moreover, many aggregates clump together into micrometer-sized agglomerates which are gradually broken up into aggregates during the mixing of the compound, yet some aggregates typically survive the mixing step. In contrast, the polymeric nanoparticles are easily dispersed in the host rubber. Given that the reinforcing carbon black aggregates are significantly larger in diameter than the cores of the nanoparticles used, the average distance (see Figure 9b) between carbon black aggregates of compound A is about 125 nm compared to 50 nm for the nanoparticle cores.

As to filler/network linkages there is no evidence for covalent linkage between nonfunctional rubber molecules and carbon black aggregates other than van der Waals bonding which induces some "bound rubber" formation. However, in the case of the polymeric nanoparticles each shell molecule is attached to the hard reinforcing core of the particle at one end. The rest of the molecule becomes entangled with the host polymer and ultimately is covalently linked to the rubber network during the vulcanization step. Thus, all the shell molecules become load holding chains if their molecular weight significantly exceeds the entanglement molecular weight. The observed greater reinforcement and superior failure properties of the nanoparticle containing compound are most likely the result of both the greater number (smaller size) of reinforcing particles and the strong covalent bonding between the host rubber and the reinforcing nanoparticle cores.

Given the highly reinforcing nature of the nanoparticles, we also investigated their use as an additive for tire compounds such as treads to increase the low strain modulus without increasing the low strain hysteresis. This is demonstrated in Figure 10, showing the storage modulus G' and tan δ a measure of hysteresis of four carbon black-filled SBR compounds. Three of the compounds contained 20 phr of polybutadienes made with different catalysts (BuLi, Ni, and Nd) and thus varying in microstructure. The fourth's compound comprised polymeric polybutadiene/styrene nanoparticles made anionically using BuLi, having a brush molecular weight of 100K and a core size of 20 nm. Even though the additional amount of reinforcing core material is only 5 phr, the shear modulus G' of the compound made with the nanoparticles increased by over 30% whereas the hysteresis remained comparable. This example illustrates that certain physical properties of rubber compounds can be modified and thus tailored by the addition of appropriately designed polymeric nanoparticles.

Concluding Remarks

We were able to reproducibly synthesize polymeric nanoparticles of different shapes based on the self-assembly into micelles of BD/S block copolymers in hexane and their form stabilization by cross-linking with divinylbenzene. Most of the nanoparticles were made on a commercially viable scale with a highly cross-linked core and an elastic high molecular weight shell structure. However, the process described also permitted the core as well as the core/shell interface to be broadly varied in composition, cross-link density, and hardness gradient. We have evidence that these structural features affect the properties of compounds prepared with such nanoparticles as they control stress transfer during deformation, and we are thus studying this effect in more detail. Using polymeric nanoparticles as reinforcing agents and performance-enhancing additives in rubber compounds showed that nanoparticles, optimally designed for this application, have a strongly reinforcing capability, a lower hysteresis response at low strains, and surprisingly strong physical properties. Changing the macrostructure of the block copolymers and process conditions also allowed us to synthesize a number of different nonspherical nanoparticles such as string-shaped, hollow, and composite nanoparticles which may provide opportunities for a broad spectrum of applications ranging from rubber composites to biomedical uses.

Acknowledgment. We are indebted to Drs. Hayes and Sadhukan for the polymer characterization and microscopy analysis of samples used in this study and thank Bridgestone Firestone for the permission to publish some of the results of this research study.

References and Notes

(1) Zilliox, J. G.; Rempp, P.; Parrod, J. *J. Polym. Sci., Part C* **1968**, *22*, 145.
(2) Bauer, B. J.; Fetters, J. *Rubber Chem. Technol.* **1978**, *51*, 406.
(3) Franta, E.; Rempp, P. *Pure Appl. Chem.* **1972**, *30*, 229.
(4) Ishizu, K.; Gramoo, S.; Fukutomi, T. *Polym. J.* **1980**, *12*, 399.
(5) Okay, O.; Funke, W. *Makromol. Chem., Rapid. Commun.* **1990**, *11*, 583.
(6) Worsfold, D. J. *Macromolecules* **1970**, *3*, 514.
(7) Tsitsilianis, C.; Chaumont, Ph.; Rempp, P. *Macromol. Chem.* **1990**, *191*, 2319.
(8) Rhein, D. H.; Rempp, P.; Lutz, P. J. *Macromol. Chem. Phys.* **1998**, *199*, 569.
(9) Eschwey, H.; Hallensleben, M. L.; Burchard, W. *Makromol. Chem.* **1973**, *173*, 235.
(10) Burchard, W.; Eschwey, H. *Polymer* **1975**, *16*, 180.
(11) Batzilla, T.; Funke, W. *Makromol. Chem., Rapid Commun.* **198**7, *8*, 261.
(12) Funke, W.; Okay, O. *Macromolecules* **1990**, *23*, 2623.
(13) Zheng, L.; Xie, A.; Lean, J. *Macromolecules* **2004**, *37*, 9954.
(14) Lui, G.; Qiao, L.; Guo, A. *Macromolecules* **1996**, *29*, 5508.
(15) Guo, A.; Lui, G.; Tao, J. *Macromolecules* **1996**, *29*, 2487.
(16) Wooley, K. L. *Chem.—Eur. J.* **1997**, *3*, 1397.
(17) Thurmond, K. B.; Kowalewski, T.; Wooley, K. L. *J. Am. Chem. Soc.* **1996**, *118*, 7239.
(18) Wooley, K. L. *J. Polym. Sci., Part A: Polym. Chem.* **2000**, *38*, 1397.
(19) Akashi, M.; Kirikihira, I.; Miyauchi, N. *Angew. Makromol. Chem.* **1985**, *132*, 81.
(20) Chen, M.-Q.; Serizawa, T.; Kishida, A.; Akashi, M. *J. Polym. Sci., Part A: Polym. Chem.* **1999**, *37*, 2155.
(21) Serizawa, T.; Takehara, S.; Akashi, M. *Macromolecules* **2000**, *33*, 1759.
(22) Garcia, C.; Zhang, Y.; Mahajan, S.; DiSalvo, F.; Wiesner, U. *J. Am. Chem. Soc.* **2003**, *125*, 13310.
(23) Krom, J.; Wang, Xr. USP6437050, 2002.
(24) Wang, Xr.; Foltz, V. J. *J. Chem. Phys.* **2004**, *16*, 121.
(25) Wang, Xr.; Foltz, V. J. Sadhukan, P. USP6689469, 2004.
(26) Wang, Xr; Foltz, V. J. USP6872785, 2005.
(27) Wang, Xr. USP6875818, 2005.
(28) Wang, Xr.; Ozawa, Y.; Hall, J. E. US Pub US2005/0154117, 2005.
(29) Wang, Xr.; Lin, C. J.; Hall, J. Warren, S.; Krom, J.; Kondo, H.; Morita, K. USP6956084, 2005.
(30) Tuzar, Z.; Kratochvil, P. Micelles of block and graft copolymers in solution. In Matjevic, E., Ed.; *Surface and Colloid Science*; Plenum Press: New York, 1993; Vol. 15, Chapter 1, pp 1−83.
(31) Hamley, I. W. In Hamley, I. W., Ed.; *The Physics of Blockcopolymers, 4*; Oxford Science Publication: Oxford, 1998; Chapters 3 and 4, pp 131−265.

MA0613739